



Diamond, Platinum-Mineral oil based Nanofluid MHD stagnation-point flow over a flat plate with heat transfer

R.SURESH^{*}, S.PALANIAMMAL^{}, M.SELVARAJ^{***}**

^{*} Department of Science and Humanities
Ambal Professional Group of Institutions
Palladam-641662, INDIA

^{**} Department of Science and Humanities
Sri Krishna College of Technology
Coimbatore-641042, INDIA

^{***} Department of Science and Humanities
Ambal Professional Group of Institutions
Palladam-641662, INDIA

Email id: rsuresh6186@gmail.com

Abstract

In this paper, we investigate the two dimensional hydromagnetic boundary layer of stagnation-point flow over a flat plate in a nanofluid with heat transfer. The governing Navier Stokes equations are reduced to a set of nonlinear ordinary differential equations using similarity transformations. The similarity equations are solved numerically by Runge Kutta Gill method for two types of nanoparticles, namely diamond and platinum with mineral oil as the base fluid. The skin friction coefficient and rate of heat transfer as well as the velocity and temperature profiles for different values of the governing physical parameters are presented graphically and discussed. Effects of the nanoparticle volume fraction on the flow and heat transfer characteristics are thoroughly analyzed.

Keywords: MHD, nanoparticle volume fraction, stagnation-point flow, Runge Kutta Gill method.



Introduction

Nanofluid is a significant factor effecting the next major industrial revolution of the current century. Many researchers have focused on modeling the thermal conductivity and examined different viscosities of nanofluid because the thermal conductivity of these fluids play an important role on the heat transfer coefficient between the heat transfer medium and the heat transfer surface. Nanofluids are now being developed for medical applications, including cancer therapy and safer surgery by cooling. Other possible areas for the application of nanofluid technology includes cooling of a new class of super powerful and small computers and other electronic devices for use in military systems, airplanes as well as for large scale cooling. To all the numerous applications must be added that, nanofluids could be used in major process industries, including materials and chemicals, food and drink, oil and gas, paper and printing and textiles. Ultra high- performance cooling is one

of the most vital needs of many industrial technologies.

The two-dimensional flow of a fluid near a stagnation-point is a classical problem in fluid mechanics. The steady flow in the neighborhood of a stagnation-point was first studied by Hiemenz⁸. Magnetohydrodynamic (MHD) boundary layer is of considerable interest in the technical field due to its frequent occurrence in industrial technology and geothermal application, high-temperature plasmas applicable to nuclear fusion energy conversion, liquid metal fluids and (MHD) power generation systems. Sparrow et al. [23] studied the effect of magnetic field on the natural convection heat transfer. Patel and Timol²⁰ studied two-dimensional MHD stagnation point flow of a power law fluid over a stretching surface. The enhancement in the thermal diffusivity values of the solvents such as ethanol, water, ethylene glycol and culture medium by the presence of gold nanoparticles have been studied by Perez²⁸ et al. Low thermal conductivity



of conventional fluids such as water and oil in convection heat transfer is the main problem to increase the heat transfer rate in many engineering equipments. To overcome this problem, researchers have performed considerable efforts to increase conductivity of working fluid. An innovative way to increase conductivity coefficient of the fluid is to suspend solid nanoparticles in it and make a mixture called nanofluid, having larger thermal conductivity coefficient than that of the base fluid. This higher thermal conductivity enhances the rate of heat transfer in industrial applications. Many researchers have investigated different aspects of nanofluids such as thermal conductivity, thermal diffusivity and viscosity of nanofluids have been studied by Kang et al.¹⁰, Velagapudi et al.²⁶, Turgut²⁵, Rudyak et al.²², Murugesan and Sivan¹⁴ and Nayak et al.¹⁵. Bachok et al. [5] studied the flow and heat transfer in an incompressible viscous fluid near the three-dimensional stagnation point of a body that is placed in a water nanofluid containing different types of nanoparticle: copper, alumina and

titania. Bachok et al. [4] also investigated two dimensional stagnation-point flow of a nanofluid over a stretching/shrinking sheet. They derived the highest values of the skin friction coefficient and the local Nusselt number were obtained for the copper nanoparticles compared with the others. Two dimensional boundary layer flow near the stagnation point on a permeable stretching/shrinking sheet in a water-based nanofluid containing two types of nanoparticles copper and silver, was studied by Arifin et al.³ Ahmad and Pop² examined the mixed convection boundary layer flow past a vertical flat plate embedded in a porous medium filled with nanofluids. Nield and Kuznetsov¹⁷ conducted the classical problems of natural convective boundary layer flow in a porous medium saturated by a nanofluids, known as the Cheng-Minkowycz's problem. Kuznetsov and Nield¹¹ investigated natural convective boundary layer flow of a viscous and incompressible fluid past a vertical semi-infinite flat plate with water based nanofluids. Mirmasoumi and Behzadmehr¹³ investigated the laminar



mixed convection of a nanofluid in a horizontal tube using two-phase mixture model. Abu- Nadu and Chamkha¹ conducted a numerical investigation on mixed convection flow in an inclined square enclosure filled with alumina-water nanofluid. Oztop and Abu-Nada¹⁹ studied natural convection in a rectangular enclosures filled with a nanofluid containing copper, alumina and titania as nano particles. They concluded that the highest value of heat transfer is obtained by using copper nanoparticles. MHD boundary layer stagnation point flow and heat transfer of a micropolar fluid towards a heated shrinking sheet with radiation and heat generation are discussed by Muhammad Ashraf and Muhammad Rashid³⁰. Kameswaran et al.³¹ discuss the effects of various material and physical parameters such as thermal radiation and nanoparticle volume fraction on heat and mass transfer characteristics in two water-based nanofluids with suction/injection and radiation and solute concentration. The effects of thermal radiation on MHD axisymmetric stagnation point flow and heat transfer of

a micropolar fluid over a shrinking sheet are studied by Shahzad Ahmad et al.³². Aurangzaib and Sharidan Shafie³³ analyzed unsteady MHD stagnation point flow with heat and mass transfer in a micropolar fluid in the presence of thermophoresis and suction/injection. Khalili et al.³⁴ discuss the unsteady magnetohydrodynamic (MHD) stagnation point flow and heat transfer of a nanofluid over a stretching/shrinking sheet is investigated numerically. The ambient fluid velocity, stretching/shrinking velocity of sheet, and the wall temperature are assumed to vary linearly with the distance from the stagnation point.

The main aim of this study is to analyze the two dimensional nonlinear steady viscous incompressible hydromagnetic boundary layer of stagnation point flow with heat transfer in a nanofluid in the presence of transverse uniform magnetic field. Utilizing similarity transform, the governing Navier-Stokes partial differential equations are reduced to set of nonlinear ordinary differential equations. The similarity equations are



solved numerically using Runge Kutta Gill method for two types of nanoparticles, namely diamond and platinum with mineral oil as the base fluid. The skin friction and rate of heat transfer as well as the velocity and temperature for different values of the

2. Mathematical formulation of the problem

Consider a steady incompressible nonlinear hydromagnetic stagnation point flow over a flat plate with heat transfer in a nanofluid in the presence of a transverse uniform magnetic field. The ambient uniform temperature of nanofluids is T_∞ , where the body surface is kept at a constant temperature T_w . The linear velocity of the flow external to the boundary layer is $U(x) = ax$, where 'a' is positive constant. Under these assumptions, the governing equations for the continuity, momentum and energy in boundary layer flow are proposed by Tiwari and Das²⁴ can be written as:

$$u_x + v_y = 0$$

$$uu_x + vu_y = UU_x + \nu_{nf} u_{yy} + \frac{\sigma_{nf} B_0^2}{\rho_{nf}} (U - u)$$

governing parameters are presented graphically and discussed. Effects of the nanoparticle volume fraction on the flow and heat transfer characteristics are also discussed.

$$uT_x + vT_y = \frac{k_{nf}}{(\rho C_p)_{nf}} T_{yy}$$

Subject to the boundary conditions

$$u = 0, v = 0, T = T_w, \text{ at } y = 0$$

$$u = U(x) = ax, T = T_\infty, \text{ as } y \rightarrow \infty$$

where u and v the velocity components along x and y axes respectively, μ_{nf} is the viscosity of the nanofluid, ρ_{nf} is the density of the nanofluid, ν_{nf} is the kinematic viscosity of the nanofluid, σ_{nf} is the electrical conductivity of the nanofluid, α_{nf} is the thermal diffusivity of the nanofluid, T is the temperature, k_{nf} is the thermal conductivity of the nanofluid and $(\rho C_p)_{nf}$ is the heat capacity of the nanofluid, which are given by Oztop and Abu-Nadu¹⁹



$$\mu_{nf} = \frac{\mu_f}{(1-\phi)^{2.5}},$$

$$\rho_{nf} = (1-\phi)\rho_f + \phi\rho_s,$$

$$(\rho C_p)_{nf} = (1-\phi)(\rho C_p)_f + \phi(\rho C_p)_s,$$

$$\frac{k_{nf}}{k_f} = \frac{(k_s + 2k_f) - 2\phi(k_f - k_s)}{(k_s + 2k_f) + 2\phi(k_f - k_s)},$$

$$v_{nf} = \frac{\mu_{nf}}{\rho_{nf}}$$

where μ_f is the viscosity of the fluid, ρ_f is the reference density of the fluid fraction, ρ_s is the reference density of $(\rho C_p)_s$ is the heat capacity of the solid, k_f is the thermal conductivity of the fluid, k_s is the thermal conductivity of the solid and ϕ is the nanoparticle volume fraction.

Introduce the following similarity variables:

$$\psi = \sqrt{av_f} xf(\eta), \quad \eta = y \sqrt{\frac{a}{v_f}},$$

$$\theta(\eta) = \frac{T - T_\infty}{T_w - T_\infty}$$

where ψ is the stream function defined

$$\text{as } u = \frac{\partial \psi}{\partial y} \quad \text{and} \quad v = -\frac{\partial \psi}{\partial x}, \quad \text{which}$$

identically satisfy Eq. (1), v_f is the

the solid fraction, $(\rho C_p)_f$ is the heat capacity of the fluid,

viscosity of the fluid, $f(\eta)$ is the stream function and $\theta(\eta)$ is the temperature.

Use the non dimensionless variables in Eq. (7), Eq. (2) to (5) reduce t with the boundary conditions

$$f(0) = 0, \quad f'(0) = 0, \quad \theta(0) = 1 \quad \text{at } \eta = 0$$

$$f'(\infty) = 1, \quad \theta(\infty) = 0 \quad \text{at } \eta = \infty$$

where



$$M = \frac{\sigma_{nf} B_o^2}{\rho_{nf} a}$$

is the Hartma

Prandtl

number

The physical quantities of interest are the skin friction coefficient c_f and the local Nusselt number Nu_x , which are defined as:

$$c_{nf} = \frac{\tau_w}{\rho_f u_w^2}, \quad Nu_x = \frac{x}{k_f (T_w - T_\infty)},$$

where

$$\tau_w = \mu_{nf} \left(\frac{\partial u}{\partial y} \right)_{y=0}$$

is the surface shear

stress and

u_w is the surface velocity

Using the non dimensional variables we get

$$\text{Re}_x^{1/2} c_f = \frac{1}{(1-\phi)^{2.5}} f''(0)$$

$$Nu_x \text{Re}_x^{-1/2} = -\frac{k_{nf}}{k_f} \theta'(0)$$

3. Numerical Analysis

The Eqs. (8) - (9) are nonlinear ordinary differential equations which constitute the nonlinear boundary value problem. As no prescribed method is available to solve nonlinear boundary value problem,

it has to be reduced to an initial value problem and then solved numerically by Runge Kutta Gill method. To initiate the process, we have to make an initial guess judiciously for the values of $f''(0)$ and $\theta'(0)$. The success of the procedure depends very much on how good the guess is. Numerical results are found for several values of the physical parameter Hartman number M , Prandtl number Pr on velocity and temperature.

4. Results and discussion

In order to get a clear insight into the problem, the numerical results for skin friction, velocity, rate of heat transfer and temperature of different values of the parameters, such as Hartman number M and the Prandtl number Pr are obtained. Table 1 indicates that the physical and thermal properties of diamond mineral oil nanofluid and platinum mineral oil nanofluid.



Table 1: Thermophysical properties of 300K base fluid and the nanoparticles at

	$\rho(kg/m^3)$	$C_p(J/kgk)$	$K(W/mk)$	$\alpha \times 10^{-7}(m^2/s)$
Mineral oil	900	2000	0.15	0.8333
Diamond	3510	500	2000	11396.011
Platinum	21470	130	70	250.797

The effect of nanoparticle volume fraction parameter ϕ on the velocity profile of platinum mineral oil nanofluid is shown in the figure 1. It is noted that the increasing values of the nanoparticle volume fraction ϕ is increase the velocity profile. This is due to the fact that the presence of nanoparticles leads to further thinning of the boundary layer. It is clear that the increasing values of nanoparticle volume fraction increases the velocity.

Figure 2 shows the effect of nanoparticle volume fraction parameter ϕ on the temperature profile of platinum mineral oil nanofluid. The presence of nanoparticle volume fraction leads to an increase in the thickness of the thermal boundary layer profile. This is because nanoparticles have high thermal

conductivity, so the thickness of the thermal boundary layer increases.

Figure 3 depicts the variation in the velocity profile for different values of Hartmann number for thorium water nanofluid. It is seen that the velocity increases with an increasing Hartmann number and consequently the thickness of the boundary layer decreases. Thus the magnetic force enhances the fluid motion in the boundary layer because the last term of the momentum equation ($U-u$) remains positive in the boundary layer region. Here the Lorentz force associated with the magnetic field makes the boundary layer thinner.

Figure 4 display the effect of magnetic parameter on the temperature profile of the thorium water nanofluid. It is clear that an increase in the magnetic



parameter decreases the temperature profile. This shows that the thermal boundary layer becomes thicker due to the effect of increasing magnetic field. Figure 5 shows the effect of nanoparticle volume fraction parameter ϕ on the velocity profile of diamond mineral oil nanofluid. It is noted that the increasing values of the nanoparticle volume fraction ϕ is decrease the velocity profile. This is due to the fact that the presence of nanoparticles leads to further thinning of the boundary layer. It is clear that the increasing values of nanoparticle volume fraction decreases the velocity.

Figure 6 display the effect of nanoparticle volume fraction parameter ϕ on the temperature profile of diamond mineral oil nanofluid. The presence of nanoparticle volume fraction leads to an increase in the thickness of the thermal boundary layer profile. This is because nano particles have high thermal conductivity, so the thickness of the thermal boundary layer increases.

Figure 7 shows the variation in the velocity profile for different values of Hartmann number for gold water nanofluid. It is seen that the velocity

Thus, the presence of the magnetic field causes the nanofluid temperature profile to decrease.

increases with an increasing Hartmann number and consequently the thickness of the boundary layer decreases. Thus the magnetic force enhances the fluid motion in the boundary layer because the last term of the momentum equation ($U - u$) remains positive in the boundary layer region. Here the Lorentz force associated with the magnetic field makes the boundary layer thinner.

The effect of magnetic parameter on the temperature profile of the gold water nanofluid is shown in the figure 8. It is clear that an increase in the magnetic parameter decreases the temperature profile. This shows that the thermal boundary layer becomes thicker due to the effect of increasing magnetic field. Thus, the presence of the magnetic field causes the nanofluid temperature profile to decrease.

Figures 9 and 10 are presented to get a clear idea about the different



nanoparticles when the base fluid is water, $\phi = 0.1$ and $M = 1$. The velocity profiles for different nanofluids are shown in figure 9. It is observed that the different nanofluids have different velocities and also noted that gold water nanofluid has higher velocity when the base fluid is water with $\phi = 0.1$ and $M = 1$ compared to thorium nanoparticle. From figure 10 it is observed that the thorium nanoparticles have the highest value of temperature profile compared to gold nanoparticles. The temperature profile of a nanofluid is based on the thermal conductivity of the nanoparticles.

The skin friction and the rate of heat transfer due to magnetic field for gold water and thorium water are depicted in figures 11 and 12 respectively. It is clear that the effect of magnetic field is to increase the skin friction whereas its effect is decrease the rate of heat transfer. Further, compared with gold water nanofluid and thorium water nanofluid, skin friction is increased for gold water nanofluid but rate of heat

transfer is decreased for gold water nanofluid.

Figure 13 is prepared to present the effect of the nanoparticle volume fraction ϕ on the skin friction coefficient $Re_x^{\frac{1}{2}} C_f$ for gold water nanofluid and thorium water nanofluid. It is found that the magnitude of skin friction coefficient increases with increasing values of nanoparticle volume fraction ϕ for both of gold water nanofluid and thorium water nanofluid. In addition, it is noted that the highest skin friction coefficient is obtained for the gold nanoparticle.

The influence of the nanoparticle volume fraction ϕ on the rate of heat transfer for different nanofluids are shown in figure 14. It is seen that the rate of heat transfer increases with increase of nanoparticle volume fraction ϕ . Moreover, it is noted that the lowest heat transfer rate is obtained for nanoparticle thorium due to domination of conduction mode of heat transfer. This is because thorium nanoparticle has the lowest value of thermal conductivity



compared to gold nanoparticle as seen in table 1. The gold nanoparticles have high values of thermal diffusivity and, therefore, this reduces the temperature gradients, which will affect the performance of gold nanoparticles.

5. Conclusion

- The magnitude of the skin friction coefficient and the rate of heat transfer increases with the nanoparticle volume fraction.
- A fixed value of the nanoparticle volume fraction ϕ , the velocity of

fluid increases by increasing Hartman number.

- A fixed value of the nanoparticle volume fraction, the temperature increases by decreasing Hartman number.
- The gold nanoparticle has the largest velocities compared to thorium nanoparticle.
- The effect of magnetic field is to increase the skin friction whereas its effect is decrease the rate of heat transfer

References

1. E. Abu-Nada and A. J. Chamkha, *Eur. J. Mech. B/Fluids*. 29, 472
2. S. Ahmad and I. Pop, *Int. Comm. Heat. Mass. Transfer* 37, 987 (2010).
3. N. Arifin, R. Nazar and I. Pop, *Sains Malays*. 40, 1359 (2011).
4. N. Bachok, A. Ishak and I. Pop, *Nanoscale Res. Lett.* 6, 623 (2011).
5. N. Bachok, A. Ishak, R. Nazar and I. Pop, *Physica B*. 405, 4914 (2010).
6. K. Bhattacharyya and G. C. Layek, *Int. Heat. Mass. Transfer* 54, 302
7. J. A. Gbadeyan, M.A. Olanrewaju and P.O. Olanrewaju *Aust. J. Basic. Appl. Sci.* 5, 1323 (2011).
8. K. Hiemenz, *Dinglers Polytech . J.* 326, 321 (1911).
9. F. Homann, *Z. Angew. Math. Mech.*
10. H. Kang, S.H, Kim and J. M. Oh, *Exp. Heat. Mass. Transfer* 19,
11. A. V. Kuznetsov and D.A Nield, *Int. J. Thermal Sci.* 49, 243 (2010).
12. T.R. Mahapatra and A. S. Gupta, *Heat. Mass. Transfer* 38, 517 (2002).



13. S. Mirmasoumi and A. Behzadmehr, *Appl. Thermal. Eng.* 28,
14. C. Murugesan and S. Sivan, *Thermal. Sci.* 14, 65 (2010).
15. A. K. Nayak, R. K. Singh and P. P. Kulkarni, *Tech. Phy. Lett.* 36, 696
16. R. Nazar, N. Amin, D. Filip and I. Pop, *Int. J. Eng. Sci.* 42, 1241 (2004).
17. D. A. Nield and A. V. Kuznetsov, *Int. J. Heat. Mass. Transfer* 52, 5792
18. P. O. Olanrewaju, M. A. Olanrewaju and A. O. Adesanya, *Int. J. Appl. Sci. Tech.*
19. H. F. Oztop and E. Abu-Nada, *Int. J. Heat. Fluid. Flow* 29, 1326 (2008).
20. M. Patel and M. Timol, *Am. J. Com. Math.* 1, 129 (2011).
21. S. R. Pop, T. Grosan and I. Pop, *Tech. Mech., Band 25. Heft 2*, 100
22. V. Y. Rudyak, A. A. Belkin and E. A. Tomilina, *Tech. Physics. Lett.*
23. E. M. Sparrow, R. D. Cess and M. Timol, *Int. J. Heat Mass. Transfer* 3,
24. R. J. Tiwari and M. K. Das, *Int. J. Heat. Mass. Transfer* 50, 2002 (2007).
25. A. Turgut, *Int. J. Thermophys.* 30,
26. V. Velagapudi, R. K. Konijeti and C. S. K. Aduru, *Therm. Sci.* 12, 27
27. J. Zhu, L. C. Zheng and X. X. Zhang, *Acta. Mech. Sin.* 27, 502
28. J. L. J. Perez, R. G. Fuentes, J. F. S. Ramirez, and A. C. Orea, *Eur. Phys. J.-Spec. Top.* 153, 159 (2008).
29. J. L. J. Perez, R. G. Fuentes, E. M. Alvarad, E. R. Gallegos, A. C. Orea, Cordova, and J. G. M. Alvarez, *Appl. Surf. Sci.* 255, 701 (2008).
30. M. Ashraf and M. Rashid, *World Applied Sciences J.* 16(10), 1338
31. P. K. Kameswaran, P. Sibanda and A. S. N. Murti, *Hindawi Publishing*
33. Aurangzaib and S. Shafie, *Indian*
34. S. Khalili, S. Dinarvand, R. Hosseini, H. Tamim, and I. Pop, *Chin.*

Fig. 1 Velocity profiles $f'(\eta)$ for different nanoparticle volume fractions for platinum mineral oil nanofluid.

Fig.2 Temperature profiles $\theta(\eta)$ for different nanoparticle volume fractions for platinum mineral oil nanofluid.

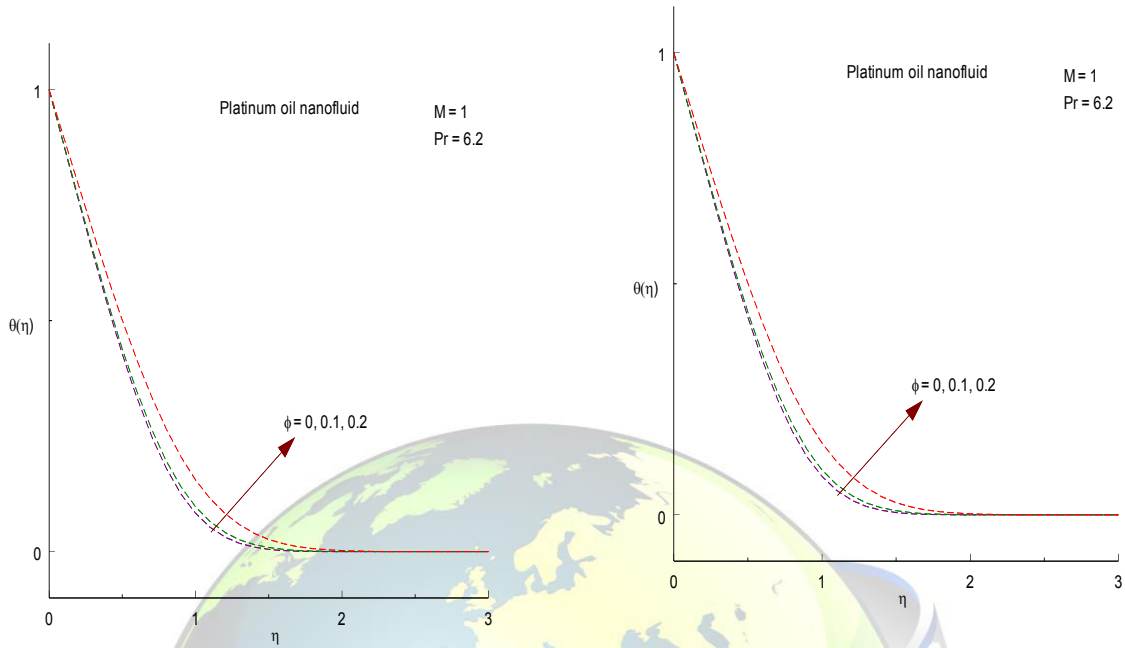


Fig. 3 Velocity profiles for different nanoparticle volume fractions for diamond mineral oil nanofluid.

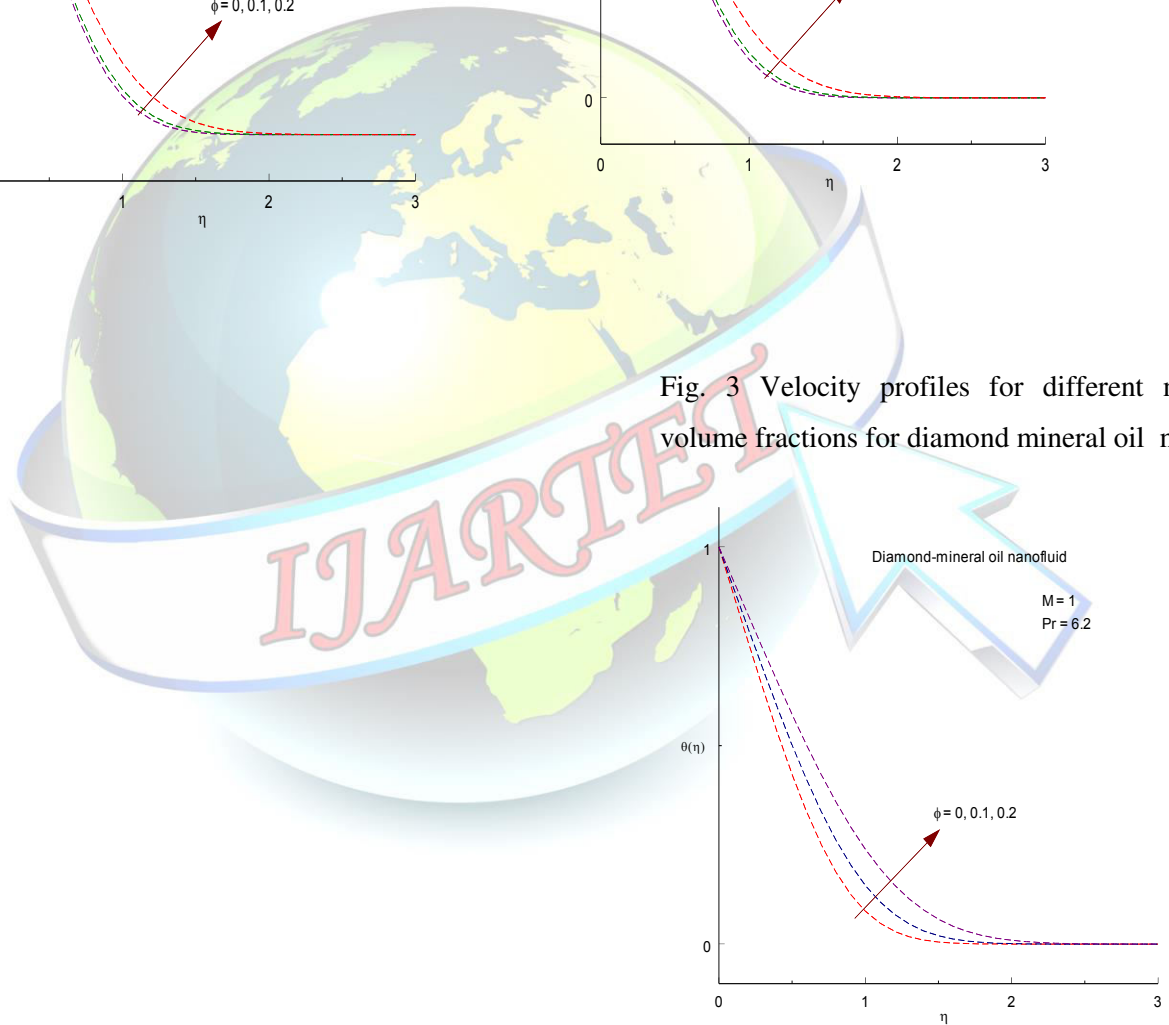




Fig. 4 Temperature profiles $\theta(\eta)$ for different nanoparticle volume fractions for diamond mineral oil nanofluid

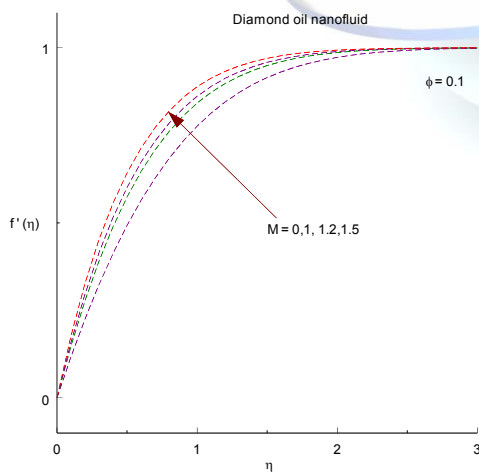
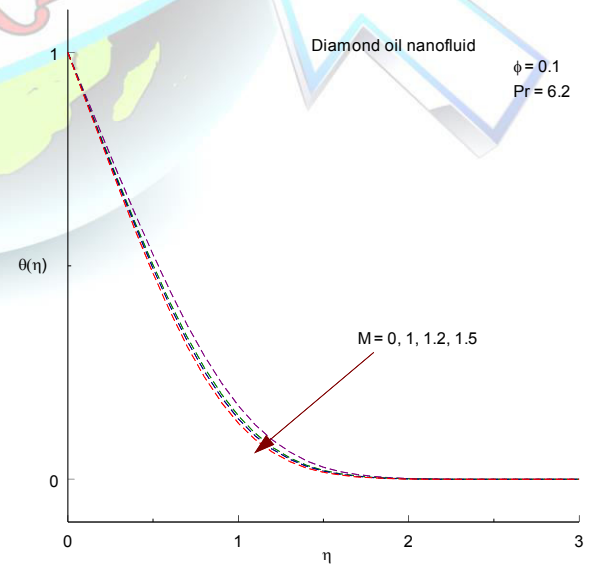


Fig. 5 Effect of the Hartman number M on the velocity profiles $f'(\eta)$ for diamond mineral oil nanofluid



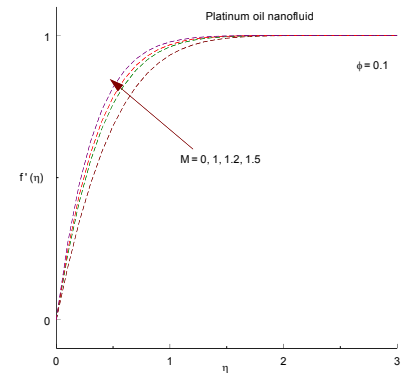


Fig. 6 Temperature profiles $\theta(\eta)$ for different nanoparticle volume fractions for diamond mineral oil nanofluid

Fig. 7 Effect of the Hartman number M on the velocity profiles $f'(\eta)$ for platinum mineral oil nanofluid

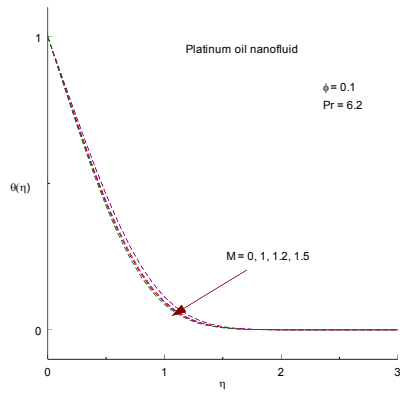


Fig. 8 Temperature profiles $\theta(\eta)$ for different nanoparticle volume fractions for platinum mineral oil nanofluid

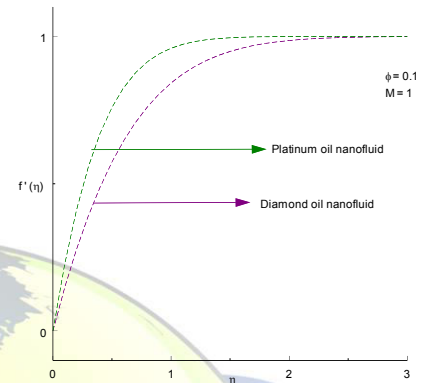




Fig. 9 Velocity profiles

$f'(\eta)$ for different nanoparticles when $\phi = 0.1$.

